A High Power Factor Pre-Regulator Control Using the DSP Controller TMS320F243

Luis Cândido Tomaselli and Hari Bruno Mohr

Instituto de Eletrônica de Potência – INEP
Departamento de Engenharia Elétrica
Universidade Federal de Santa Catarina – UFSC
Cx. Postal 5119 – 88040-970 Florianópolis (SC) – Brasil
hari@inep.ufsc.br

***Abstract* – This work deals with a study of a boost converter operating as a high power factor pre-regulator using the DSP controller TMS320F243 from Texas Instruments. The study begins with a description of the controller. Afterwards, the control circuit of the converter is described. The results obtained by simulation and experimentation are presented for a prototype implementation with an output voltage equal to 400V, an output power equal to 500W and a switching frequency equal to 50kHz.**

I. INTRODUCTION

The pre-regulator with high power factor is present in several industrial and commercial applications. The most employed topology for this purpose is the boost converter. Its advantage lies in the fact that the input current isn't pulsed, which reduces the amount of harmonics injected in the AC line. The digital control of a boost converter operating as a pre-regulator with high power factor is studied.

The digital control, although being a well-known subject since the middle of the last century, plays a very important part inside power electronics. Nowadays several control forms in commercial products can be implemented through the DSPs cores, which were only present before in high technology laboratories or in simulation software. The current processing capacity allows the execution of a lot of tasks, which were limited before. Therefore, digital control is an attractive option.

A DSP is basically an optimized microprocessor used to perform mathematical processing, while other processors are optimized for manipulation and management of data. This feature enables it to work with applications that do not tolerate significant delay times between the digital data acquisition, calculations and the return of digital data as an answer. The DSP controller used here has a unique characteristic of containing just one-package controller peripherals and the mathematical processing necessary to a pre-regulator prototype with high power factor. It allows the designers to implement multiple functions such as serial communication, analog-to-digital conversion, parallel communication, timers, PWM, etc. The DSP also allows the construction of a universal platform to control several power supplies with different parameters (power rating, voltage, current, etc) making it necessary only to change parameters in the algorithm. However it can have its viability refuted in some specific cases due to economical factors.

In this project a fixed-point controller with Harvard internal architecture, TMS320F243, was used [1-4]. The DSP controller's main characteristics are:

- Module event manager;
- Eight compare/pulse width modulation (PWM) channels;
- Two 16-bit general purpose timers with four operation modes;
- A pseudo-dual 10-bit analog-to-digital converter;
- 26 individually programmable, multiplexed I/O pins;
- Phase-Locked loop (PLL) – based clock module;
- Watchdog (WD) timer module with real-time interrupt (RTI);
- Memory:
  - 544 words x 16 bits of on-chip data/program dual access RAM;
  - 8k words x 16 bits of on-chip memory FLASH EEPROM or ROM;
  - 224k words x 16 bits of maximum addressable memory space.

The implemented control of the pre-regulator was based on the method used by UC3854 integrated circuit, applying the correct considerations due to the effect of sampling the controlled and monitored variables and analyzing discrete time techniques. The project method of the boost converter (as a pre-regulator) for average value control mode is already part of the scientific and industrial communities' knowledge and they are widely studied and presented in several publications [5-12].

The goals of this work are to present a general vision of the adopted procedure, the organization of the program, the simulation results and the prototype results for a boost converter of 500W and 50kHz.

II. SYSTEM CONTROL DESCRIPTION

Differing from the continuous controller [5-12], considered as the base of this project, it was preferred to impose the waveform starting from a table of points in

the program memory of DSP controller. In this way there is a reference that is independent from the input voltage and is roughly sinusoidal (a small distortion exists, due to its discrete nature). In order to synchronize the look sine table contained in the DSP (Digital Signal Processor) internal memory with the input line voltage, the zero crossing point was detected in the input line voltage. At that moment the pointer of the table was restarted.

In the conventional controller the voltage waveform of the AC line is used, which can present a distortion in its format, which is extended to the input current, decreasing the power factor. Another point is that, using the voltage of the AC line as a reference, it is necessary to calculate the square of the average value of the input voltage to compute the feedforward action, which implicates an increase of the program complexity. In this case, since the reference for current format is independent from the AC line, there is no need to calculate the square for the correction action.

To calculate the action of feedfoward, the average value of the voltage of rectified input was calculated. For the continuous controller, it is done in the same way. However, by means of second order filter that always has a ripple. This ripple is reflected in the format of the input current, increasing the harmonic distortion (THD) of current. This influence is reduced by using the calculated average value and by updating each semi-cycle (during the zero crossing).

Since controlling the average value of the output voltage is desirable, it was calculated and controlled, instead of using the instantaneous value.

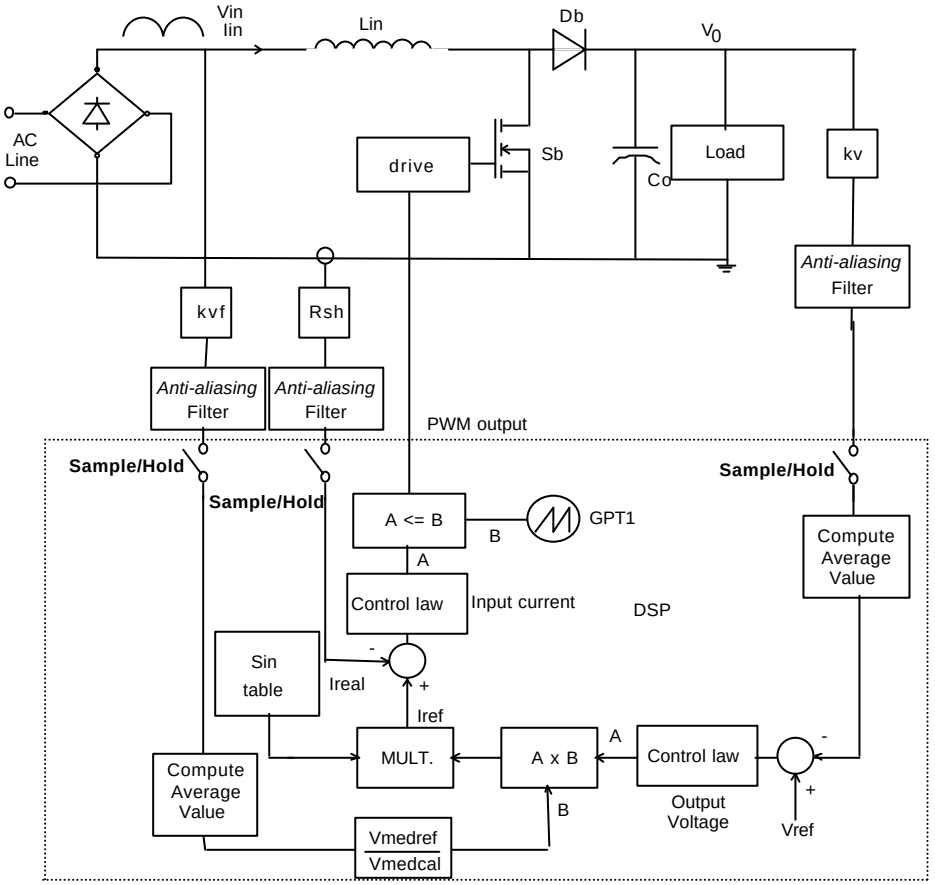

Fig. 1 - Functional block diagram of the control implemented with the DSP controller.

The project of the controller is divided in two fundamental parts. The first one consists of obtaining a mathematical model that describes the process and that can be used for the analysis and to project the controller. A method for modeling the converter using the model of the PWM switch proposed by Vorperian [13] was used. Through this method, a model of the plant or process is obtained and a discretization method is used to find the equivalent model in the z domain. The second part includes the project of the controller that allows the plant to comply with the desired specifications.

Basically, there are two forms of projecting a digital controller. One of them is by approximation; this consists of a project of the compensator in the s domain, upon conclusion, a discretization method [14] (Method of Tustin, etc) is used to obtain the transfer function in the z domain.

The other method is analytical, based on the tools of the project in the s domain applied to the discretized transfer function [14]. It tends to be more accurate than the methods by approximation. This method was the chosen one for the project of the compensator. The

sample rate was 50kHz. Furthermore, the sample rate of voltage loop was 120Hz (the mean value was controled). Using a frequency method project (Bode), the following discrete control laws for the current loop (1) and for the voltage loop (2) were reached.

$$u(k) = u(k-1) + 0{,}44 \times e(k) - 0{,}3198 \times e(k-1) \quad (1)$$

$$u(k) = u(k-1) + 0{,}78 \times e(k) - 0{,}74 \times e(k-1) \quad (2)$$

A problem in the implementation of these laws lies in their numerical representations. As there is a definite number of patterns, it is necessary to study which is the best format to use, so that the error in the representation and of calculations are minimized. In the fixed-point processors, the number of existent patterns, in a certain way, introduces noise in the treated signs. However, DSPs present an architecture that increases the signal/noise relation during processing, favoring the perfect adjustment in control applications, as this one. The representation format adopted was chosen in a way to increase the signal/noise relation. This way, the program works with different radixes to obtain better accuracy.

III. SIMULATION RESULTS

A choice for the use the state equations of the boost converter was made. Notice that the variables to be controlled are exactly the state variables of the system. Since the main purpose here is to test the control laws; the model of the converter used is obtained via the state equations [15]. The following simplified hypothesis were assumed to obtain the proposed model:

- The conduction resistance of the diode and the switch are zero and the resistance when switched off is infinite;
- The converter always works in the continuos mode;
- The intrinsic parameters of the components are not considered;
- The state variables chosen are the average current of the input inductor and the average voltage in the output capacitor;
- A switching function was considered (q(t)), which assumes two possible values: one (1) when the switch is conducting and the diode is blocked; and zero (0) when the switch is blocked and the diode is conducting. The mean value of q(t) during a commutation period is called duty cycle (D).

Considering that these conditions are satisfied, the operating stages are then presented in Fig. 2. Thus, the following expressions are obtained:

$$\frac{diL(t)}{dt} = \frac{1}{Lin} \times \left(vin(t) - vc(t) \times \left(1 - q(t)\right)\right) \quad (3)$$

$$\frac{dvc(t)}{dt} = \frac{1}{C_0} \times \left(iL(t) \times \left(1 - q(t)\right) - \frac{vc(t)}{R_0} \right) \quad (4)$$

$$v_0(t) = vc(t) \quad (5)$$

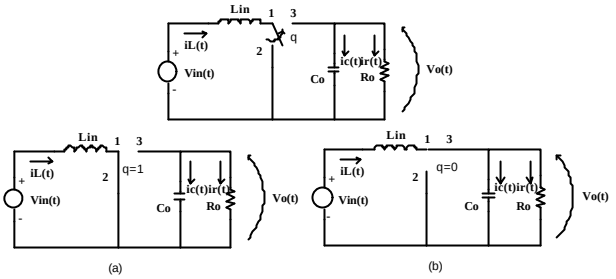

Fig. 2 – Operating stages of the buck-boost converter.

As an initial step, these equations make the study of the control laws behavior possible. If the simulator flexibility allows the use of fixed-point logic, the dynamic behavior can be verified for different radixes and from this analysis, the most adequate format is chosen. Some results obtained by simulation using fixed-point logic blocks are presented.

In order to perform such studies a project and a prototype with the following characteristics were done:

- Line voltage (Vin_{RMS}): 90 – 250V.
- Output power (P_0): 500W.
- Frequency line (f_r): 60 Hz.
- Output voltage CC (V_0) – 400V.
- Output ripple voltage (ΔV_0): ±2,5% de V_0.
- Output ripple current (ΔIn_{max}): 20% de IL_{IN}.
- Switching frequency (f_s): 50kHz.
- Sample frequency (f_a): 50 kHz.
- Efficiency (η): 95%.
- L_{in} = 1,3mH
- C_o = 470μF

Fig. 3 shows the dynamics of the output voltage after a 30% disturbance in the load and a line voltage drop from 220V to 120V. As mentioned before, one can notice that the controller maintains the output voltage inside of the desired value range. The overshoot was around 10% and the settling time was around 300ms. The input current behavior is also presented. It can be seen that with an input voltage disturbance the system's dynamics is faster than with a load disturbance. The input voltage was presented in order to show when the disturbance was applied.

Fig. 4 shows a zoom in Fig. 3. It can be noticed that both the current waveform and the output voltage mean value are in agreement with the desirable values.

Fig. 5 shows the current and voltage controllers output, as one can notice that they don't saturate. Fig. 6 shows a zoom in Fig. 5. It can be noticed that their behavior was in agreement with the theoretical values.

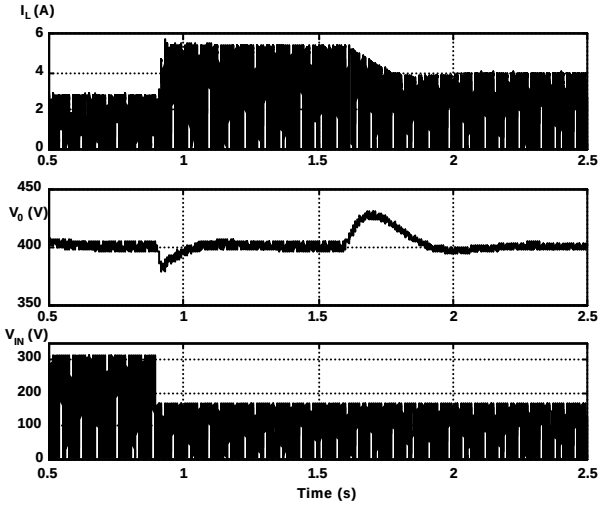

Fig. 3 – Output voltage, input current behavior with disturbances in the line voltage (waveform at the bottom) and in the load (30%).

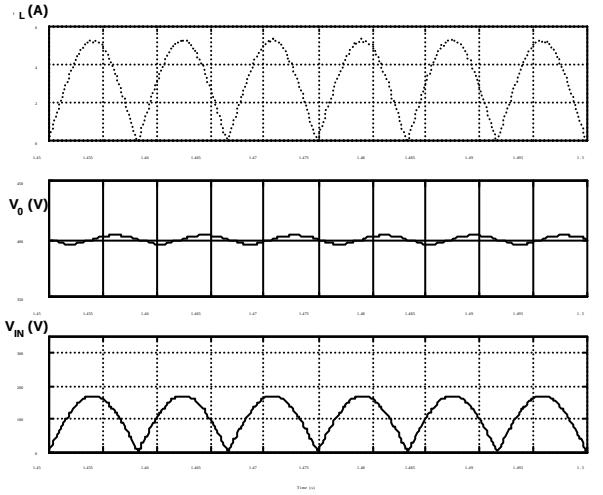

Fig. 4 – Zoom in the output voltage, input current behavior with disturbances in the line voltage (waveform at the botton) and in the load (30%).

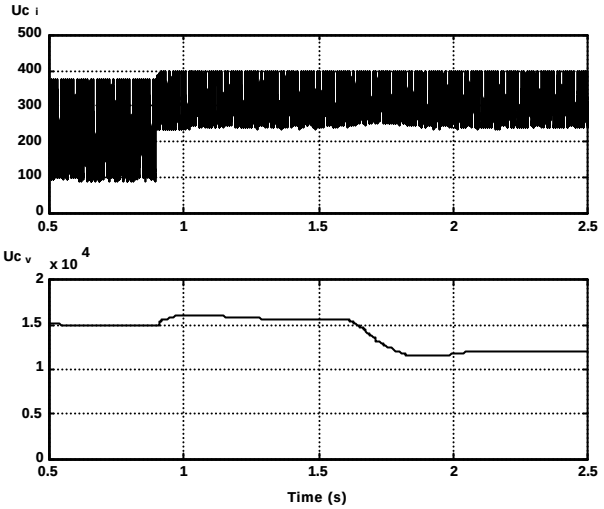

Fig. 5 – Action controllers behavior.

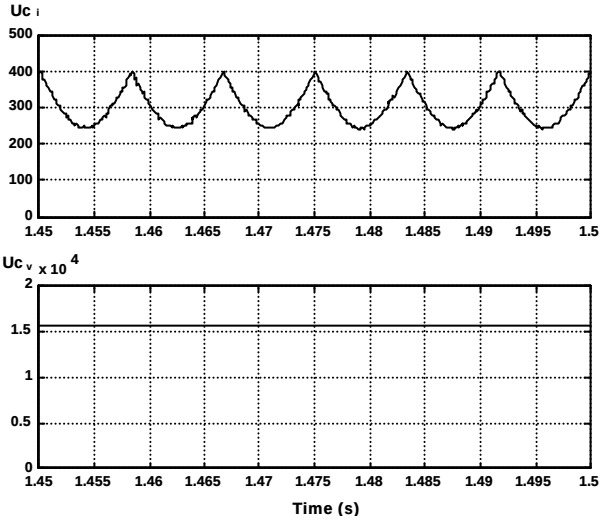

Fig. 6 – Zoom in the controllers action.

Fig. 7 shows the boost converter scheme.

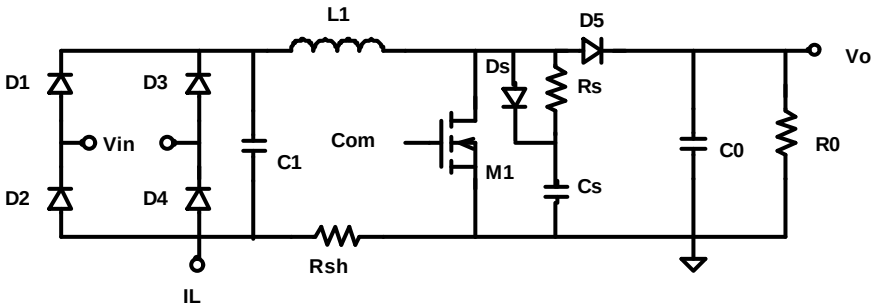

Fig. 7 – Boost converter scheme.

IV. EXPERIMENTAL RESULTS

Fig. 8 and Fig. 9 show the waveforms of the input voltage and current for a nominal load and different RMS input voltages. It can be noticed that the current has its waveform imposed by the reference and the output power is constant, as desired; however, with the decrease of the current, the THD increases as in analog controllers.

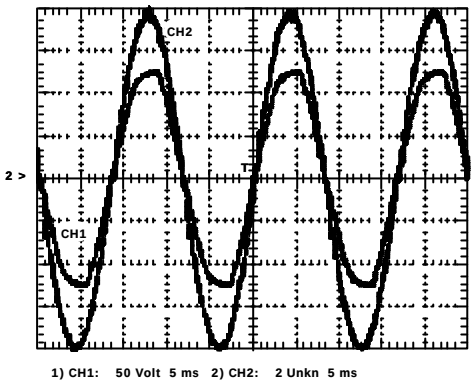

Fig. 8 –Input voltage (CH1) and input current (CH2) of the boost converter.

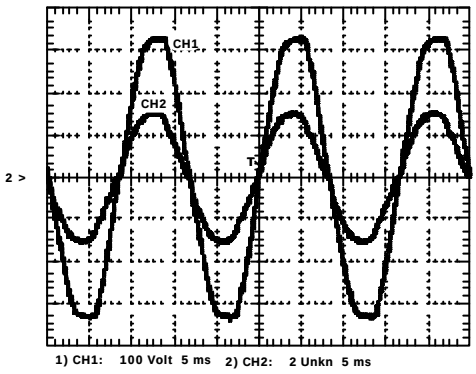

Fig. 9 - Input voltage (CH1) and input current (CH2) of the boost converter.

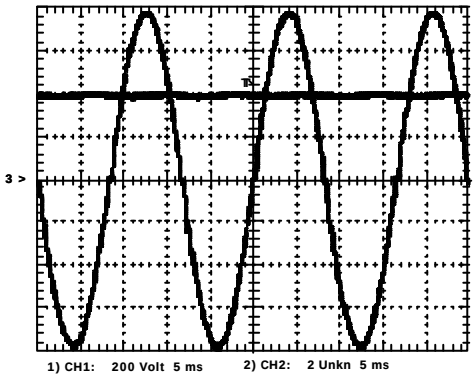

Fig. 10 – Output voltage (CH1) and input current (CH2) for Vin = 90V.

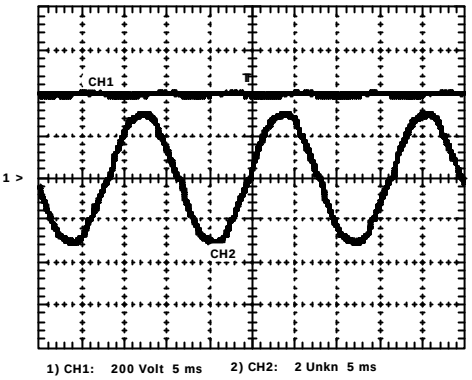

Fig. 11 - Output voltage (CH1) and the input current (CH2).

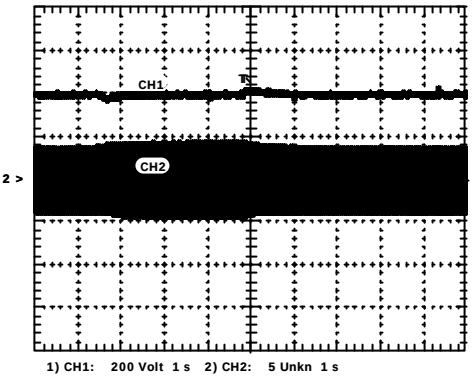

Fig. 12 – Output voltage (CH1) and input current (CH2) with a 30% disturbance in the load.

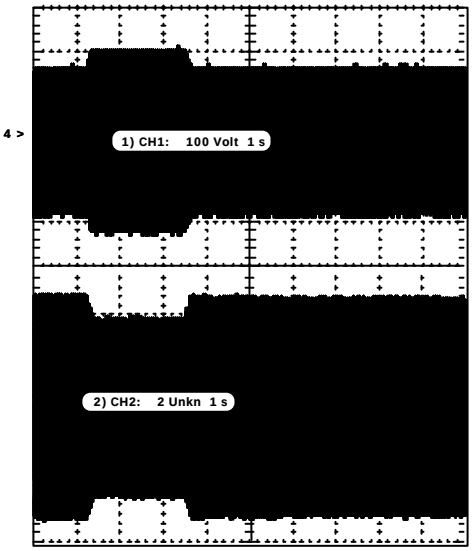

Fig. 13 - Input voltage (CH1) and input current (CH2) with a 20% disturbances in line voltage.

Fig. 10 and Fig. 11 show the output voltage for a nominal load and different input line voltages. It can be noticed that the output voltage is regulated at 400V.

A notion of the system behavior is shown in Fig. 12 and Fig. 13.

Fig. 12 shows the behavior of both output voltage and current for a 30% decrease in the nominal load and when the load was increased to reach the nominal load again. It can be noticed that the transitory time and the output voltage overshoot values are in agreement with the simulation performed with the converter model that employs state equations. The overshoot was around 40V and the settling time was around 300ms.

Fig. 13 presents the results obtained with the input voltage variation.

TABLE I
THD$_I$, THD$_V$ AND POWER FACTOR BEHAVIOR WITH THE INPUT VOLTAGE RMS VALUE.

V_{ef} (V)	THD_i	THD_v	P.F.
90	2,35%	4,32%	0.998792
110	2,02%	3,98%	0.999005
130	1,77%	3,84%	0.999107
140	1,84%	3,76%	0.999125
160	2%	3,66%	0.999131
170	2%	3,66%	0.999131
200	2,71%	3,66%	0.998964
220	3,2%	3,7%	0.998805
240	4,15%	3,79%	0.998423

Table I shows the THD measurements for different input voltage RMS values and the corresponding power factor. The worst case was verified when the input voltage was 240V_{RMS}. It can be noticed that the results are in compliance to IEC 61000-3-2 standard [16].

V. CONCLUSION

A study of a digital controller for a boost converter was presented. The employed controller was a DSP using fixed-point logic. The radixes logic was used. This is an important feature in the design, because the better the choice of the radixes, the better the final response of the system. A wrong choice could cause an unexpected behavior of the controller and overall system.

The main advantages of digital controllers are fault protections, communication protocols, etc, which could be implemented. Another advantages are the possibility of modifying the entire control scheme just by changing the instructions, and the possibility of having a universal control circuit board for many converters, which would reduce the manufacturing price. A disadvantage lies in his economical viability, that can be refuted in some cases.

VI. REFERENCES

[1] *Spectrum Digital Symbolic Assembler for the F24X DSP*, Technical Reference, DSP Development Systems, Houston, 1999.

[2] *TMS320C2XX Fixed Point Assembly Language Users Guide*, Technical Reference, Texas Instruments, Houston.

[3] *TMS320F243, TMS320F241 DSP Controlers*, Technical Data Sheet, Texas Instruments, Houston, 1999.

[4] TMS320F243/F241/C242 *DSP Controlers Reference Guide – System and Peripherals*, Technical Reference Guide, Texas Instruments, Houston, 1999.

[5] GROSSE, ALEXANDRE S.. *Controle de um Pré-regulador com Alto Fator de Potência Utilizando Microcontrolador PIC*. Dissertação de mestrado. UFSC, Florianópolis , 1999.

[6] HELDWEIN, MARCELO L.. *Unidade Retificadora Trifásica de Alta Potência e Alto Desempenho para Aplicação em Centrais de Telecomunicações*. Dissertação de mestrado. UFSC, Florianópolis , 1998.

[7] BARBI, IVO; SOUZA, ALEXANDRE F.. *Correção de Fator de Potência de Fontes de Alimentação*. Apostila – Publicação Interna INEP/EEL. UFSC, Florianópolis , 1995.

[8] SOUZA, ALEXANDRE F. *Retificadores Monofásicos de Alto Fator de Potência com Reduzidas Perdas de Condução e Comutação Suave*. Tese de doutorado. UFSC, Florianópolis , 1995.

[9] JUNIOR, ELIAS T. S.. *Análise e Projeto de Compensadores para o Conversor Boost*. Dissertação de mestrado. UFSC, Florianópolis , 1994.

[10] DIXON, LLOYD. *Average Current Mode Control of Switching Power Supplies*. Application Note U-140. Unitrode. http://www.ti.com, 2000.

[11] TODD, PHILIP C.. *UC3854 Controled Power Factor Correction Circuit Design*. Application Note U-134. Unitrode. http://www.ti.com, 2000.

[12] TODD, PHILIP C.. *UC3854 Controlled Power Factor Correction Circuit Design*. U-134, Application Note, Unitrode, 1990.

[13] VORPERIAN, V.. "Simplified Analysis of PWM Converter Using the Model of the PWM Switch", VPEC Seminar Tutorial, Sep. 1989.

[14] OGATA, KATSUHICO. *Discrete-Time Control Systems*. Second Edition. Prentice Hall, Englewood Cliffs, New Jersey , 1994.

[15] VERGHESE, GEORGE C., TAYLOR, DAVID G., JAHNS, THOMAS M. & DE DONCKER, RIK W.. *The Control Handbook – Cap. 78 - Power Eletronics Control*. CRC Press, Inc. 1996.

[16] IEC 61000-3-2, Eletromagnetic compatibility (EMC) Part 3-2: Limits for harmonic current emissions (equipment input current ≤ 16 A per phase). International Electrotechnical Commission. Ed. 1.2, 1998-04.